JACS
JOURNAL OF THE AMERICAN CHEMICAL SOCIETY
Article
Cite This: J. Am. Chem. Soc. 2018, 140, 1116−1122
pubs.acs.org/JACS

Reticular Electronic Tuning of Porphyrin Active Sites in Covalent Organic Frameworks for Electrocatalytic Carbon Dioxide Reduction

Christian S. Diercks,[†,‡,§,⊥] Song Lin,[†,‡,∥,∥] Nikolay Kornienko,[‡] Eugene A. Kapustin,[‡,§,⊥] Eva M. Nichols,[‡,∥] Chenhui Zhu,[▽] Yingbo Zhao,[‡,§,⊥] Christopher J. Chang,*[,‡,∥,#] and Omar M. Yaghi*[,‡,§,⊥]

[‡]Department of Chemistry, [§]Kavli Energy NanoSciences Institute and Berkeley Global Science Institute, and [#]Howard Hughes Medical Institute, Department of Molecular and Cell Biology, University of California, Berkeley, California 94720, United States
[∥]Chemical Sciences Division, [⊥]Materials Sciences Division, and [▽]Advanced Light Source, Lawrence Berkeley National Laboratory, Berkeley, California 94720, United States
[∥]Department of Chemistry and Chemical Biology, Cornell University, Ithaca, New York 14853, United States

Supporting Information

ABSTRACT: The electronic character of porphyrin active sites for electrocatalytic reduction of CO_2 to CO in a two-dimensional covalent organic framework (COF) was tuned by modification of the reticular structure. Efficient charge transport along the COF backbone promotes electronic connectivity between remote functional groups and the active sites and enables the modulation of the catalytic properties of the system. A series of oriented thin films of these COFs was found to reduce CO_2 to CO at low overpotential (550 mV) with high selectivity (faradaic efficiency of 87%) and at high current densities (65 mA/mg), a performance well beyond related molecular catalysts in regard to selectivity and efficiency. The catalysts are stable for more than 12 h without any loss in reactivity. X-ray absorption measurements on the cobalt L-edge for the modified COFs enable correlations between the inductive effects of the appended functionality and the electronic character of the reticulated molecular active sites.

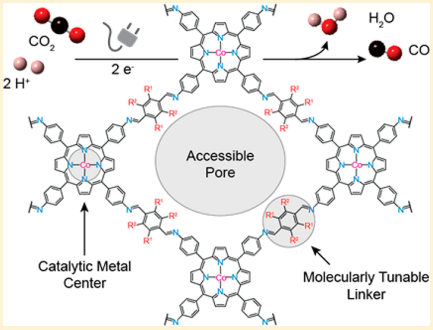

INTRODUCTION

Covalent organic frameworks (COFs) are composed of covalently linked organic molecules, which are held together in specific geometric and spatial arrangements.[1−5] Research efforts have largely focused on varying the size and shape of the molecular building blocks to design the structural properties of COFs such as porosity.[6−15] In this report, we show how these building blocks can also be tuned electronically such that remote functionalization of linker units has a significant impact on the electronic character of molecular active sites embedded within the reticular superstructure and consequently, their accompanying reactivity. Within this context, we and others have recently identified COFs and their related MOF congeners as a promising platform for supporting molecular catalysts for the electrochemical conversion of carbon dioxide to carbon monoxide.[16−18] Indeed, extensive research has been devoted to the design of molecular catalysts that facilitate this chemical transformation, and while electrolytic approaches benefit from using water as a reaction medium that facilitates proton and electron transfer, its use also requires good selectivity of the catalyst over the competitive off-pathway reduction of water itself to hydrogen.[19−29] Consequently, systems used for this transformation must be tuned for both high reactivity and selectivity.[24,30−36] Molecular CO_2 reduction catalysts have been optimized in terms of activity and selectivity by functionalization of the organic ligands on the catalytically active metal center, as illustrated by extensive work on metalloporphyrin systems as a prime example.[37−43] Indeed, the direct functionalization of the porphyrin building block is synthetically challenging through such a pure molecular approach. We reasoned, however, that the high charge carrier mobility of COF-366-Co would allow for electronic communication throughout the whole framework of the material and thus hypothesized that we can therefore circumvent the direct modification of the porphyrin building-block and instead functionalize the organic strut that is used to reticulate it into the extended framework. It is worthy of note that the potential for remote functionalization is advantageous in the context of the rational optimization of CO_2 electroreduction catalysts because it reduces the influence of the introduced functionality to electronic effects and potentially circumvents undesirable interference in the reaction via steric hindrance or through non-covalent interactions.

As a first step, we synthesized a series of COFs with different electron withdrawing groups on their respective struts termed

Received: November 16, 2017
Published: December 29, 2017

DOI: 10.1021/jacs.7b11940
J. Am. Chem. Soc. 2018, 140, 1116−1122

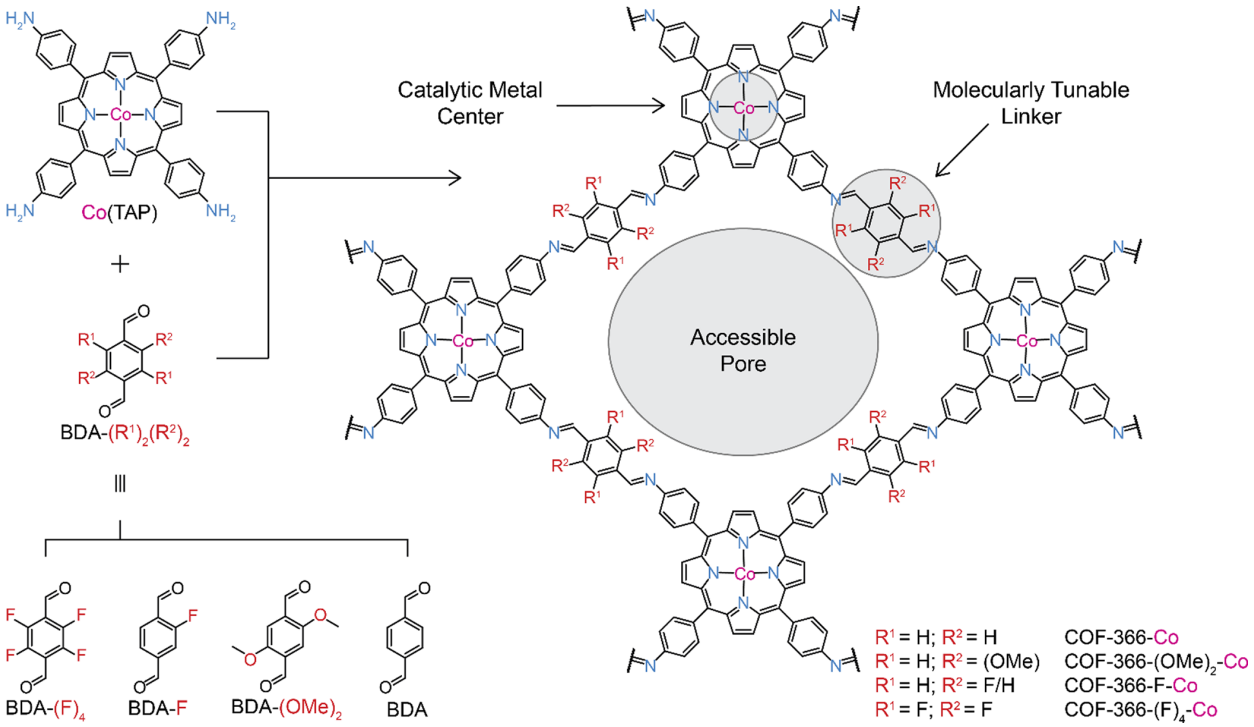

Figure 1. Design and synthesis of cobalt-porphyrin derived covalent organic frameworks. The molecular nature of the COF backbone allows for systematic modulation of the electronic structure of the catalytically active cobalt center. Because of the porosity of the framework diffusion of the reactants to the active sites is facilitated.

COF-366-Co, COF-366-$(OMe)_2$-Co, COF-366-F-Co and COF-366-$(F)_4$-Co (Figure 1; Section S1). To make a comparison between the aforementioned materials in terms of reactivity, two critical points had to be addressed. First and foremost, when deposited on the electrode as a microcrystalline powder, only a small amount of the COF is electrochemically accessible.[44] As such, to better compare the reactivity of the different samples, we prepared thin films of the materials to ensure that the majority of the metal centers in the framework are electrochemically active. Second, to rationally design a catalyst it is important to monitor the effect of the functionalization on the electronic structure of the active site. Because the orbitals that are primarily relevant to the catalytic activity of the cobalt centers are its 3d orbitals, we decided to investigate the cobalt L-edge X-ray absorption spectroscopy (XAS) data of the functionalized COFs to assess inductive effects of the reticular structure. These transitions consist of excitation of 2p core electrons into empty 3d-orbitals. Indeed, we observe that functionalization of the struts with electronegative elements directly translates into an electron withdrawing effect on the cobalt center and the extent of this effect is proportional to the electronegativity, as well as the amount of functional groups that are installed. The observed differences in electronics significantly alter the reactivity of the molecular active sites in the reticular material, which can be rationalized based on the proposed mechanism for the electrocatalytic reduction of CO_2 to CO using cobalt porphyrin derived catalysts. This report represents a study of direct electronic structure–function relationships of COF electrocatalysts.[45]

EXPERIMENTAL SECTION

COF Synthesis. A Pyrex tube measuring 10 × 8 mm (o.d × i.d.) was charged with 5,10,15,20-tetrakis(4-aminophenyl)porphinato]-cobalt [Co(TAP)] (18 mg, 0.025 mmol), BDA, 2,5-dimethoxyterephthaldehyde/2-fluoroterephthaldehyde/2,3,5,6-tetrafluoroterephthaldehyde (0.075 mmol), 1,2- dichlorobenzene (1 mL), butanol (1 mL), and 6 M aqueous acetic acid (0.25 mL). After sonication for 15 min the tube was flash frozen at 77 K (liquid N_2 bath). After one freeze–pump–thaw cycle the system was evacuated to an internal pressure of 50 mTorr and flame-sealed. The reaction was heated at 120 °C for 72 h, yielding a dark purple precipitate at the bottom of the tube, which was isolated by filtration. The wet sample was then transferred to a Soxhlet extractor and thoroughly washed with methanol (24 h) and acetone (24 h). Following that, the product was washed five times with liquid CO_2. The system was then heated up to 45 °C to bring about the supercritical state of CO_2 and slowly bled to ambient pressure. Finally the product was evacuated at 100 °C for 18 h at 1×10^{-2} mtorr to yield activated sample. Yield: 24.18 mg, ~90% based on Co(TAP). For the synthesis of the thin films an HOPG substrate was added to the synthesis conditions described above. Upon completion of the reaction, the substrate was separated from the bulk COF, sonicated briefly, and washed over 2 days with acetone and methanol in a 20 mL vial.

X-ray Absorption Spectroscopy. XAS data was acquired at beamline 6.3.1 at the Advanced Light Source in Lawrence Berkeley National Lab. Samples were prepared for measurement by lightly pressing a thin film of the desired sample onto a conductive copper or carbon substrate prior to loading into the measurement chamber. The X-ray source was 1.9 GeV with a current of 500 mA. L-edge energy calibration was performed with a metallic cobalt foil standard. All samples were measured in an ultrahigh vacuum (UHV) environment of 1×10^{-9} Torr and 300 K. The monochromator slit width was decreased to the smallest possible value to simultaneously decrease photon flux incident on the sample of interest and to obtain the highest possible energy resolution. For our chosen parameters, the

DOI: 10.1021/jacs.7b11940
J. Am. Chem. Soc. 2018, 140, 1116–1122

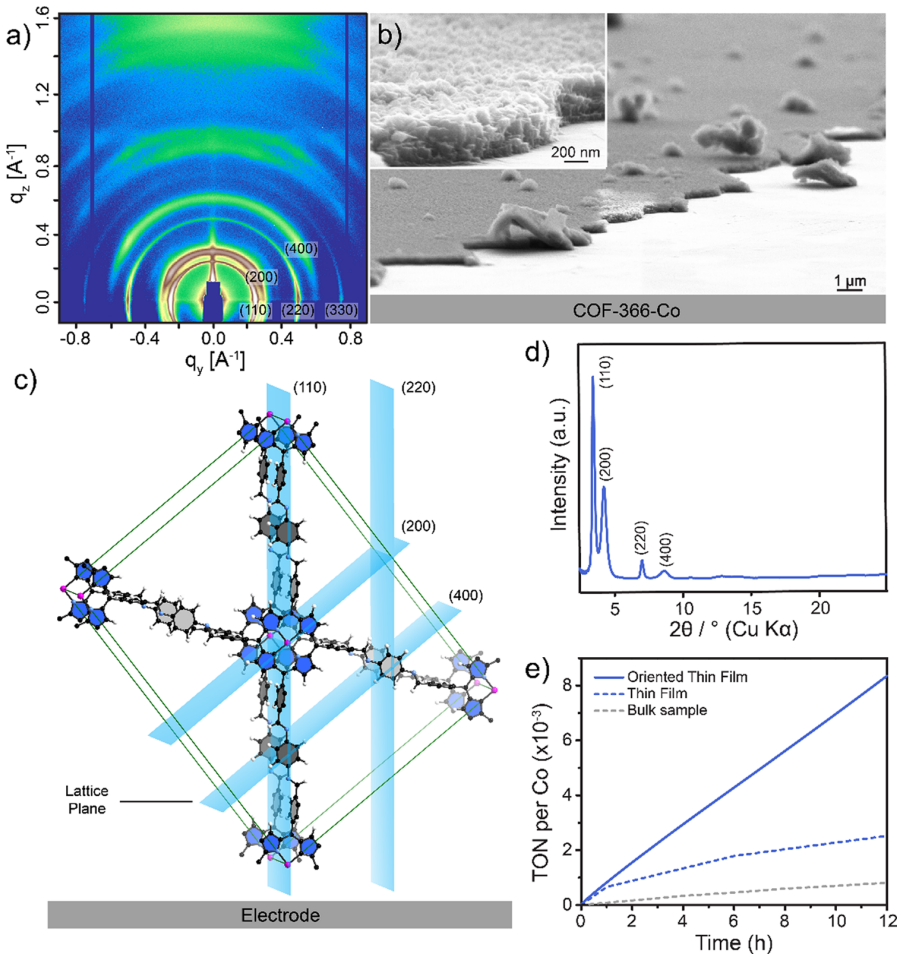

Figure 2. Optimizing the morphology of the COF catalyst. (a) Grazing incidence wide-angle X-ray scattering (GIWAXS) of the COF film on HOPG shows preferred orientation of the material. (b) COF forms uniform films of 250 nm in thickness as shown by SEM. (c) Data suggest that the COF layers are oriented in a 90° angle with respect to the substrate. (d) 2D line-profile of the GIWAXS data is in good agreement with the expected diffraction pattern. (e) Oriented thin films of COF-366-Co outperform deposited COF on porous carbon fabric and films without preferred orientation obtained on glassy carbon.

resulting energy resolution was measured to be 0.6 eV. X-ray induced damage was carefully monitored for. Each experimental spectrum consists of >6 individual spectra taken at different spots of the sample on the stage. Before each individual high-resolution spectrum was taken, a fast survey scan was also taken on the same sample spot. The high-resolution and survey spectra were closely compared to determine that the X-ray beam did not damage the COF and change the resulting spectrum.

Cobalt L-edge spectra were simulated with CTM4XAS software.[46] A reasonable set of starting parameters was obtained through a survey of the literature. D4h symmetry, Co^{2+} formal oxidation state, 1.6 eV 10Dq, 300oK, 0.95 spin orbital coupling, 0.2 eV Lorentzian broadening, and 0.2 eV Gaussian broadening parameters were consistent for simulations across all samples. The effects of electron-withdrawing and -donating groups were simulated through the variation of the Slater integral parameters from 0.6 to 1.1.

Electrochemistry. For the electrolysis experiments, 0.5 M potassium bicarbonate was used as the electrolyte. A standard 3-electrode setup was employed with a carbon disk counter electrode and Ag/AgCl reference electrode. For product quantification, a home-built two-compartment setup was used which featured a nafion membrane separating the working and counter compartments. GC analysis was performed at each time point by direct introduction of the headspace into a GC sampling loop. All current densities are normalized by amount of cobalt as determined by inductively coupled plasma atomic emission spectroscopy (ICP).

GIWAXS. Grazing incidence wide-angle X-ray scattering data were acquired with a Pilatus 2 M detector (Dectris) instrument on beamline 7.3.3 at the Advanced Light Source, Lawrence Berkeley National Laboratory (λ = 1.24 Å). The incidence angle was held at 0.120 to optimize signal collection. Silver behenate was used to calibrate the sample−detector distance and the beam center. The Nika package for IGOR Pro (Wavemetrics) was utilized to reduce the acquired 2D raw data to 2D images in reciprocal space and convert 2D images to 1D line profiles.[47]

RESULTS AND DISCUSSION

Oriented Thin Films of COF-366-Co. Our initial efforts were directed toward the optimization of the electrochemical accessibility of the COF catalyst by controlling the morphology of the system. One major drawback of our initial system was that only a small portion, 4−8%, of the cobalt sites were in fact electrochemically accessible which we attributed to the poor contact of the sample with the electrode surface and sluggish transportation between individual COF crystallites.[16] As such, we chose to move from depositing the microcrystalline COF

DOI: 10.1021/jacs.7b11940
J. Am. Chem. Soc. 2018, 140, 1116−1122

powder onto porous carbon fabric toward directly growing thin films of COF onto the electrode surface. In our first attempt, we tried to grow COF-366-Co on glassy carbon. While these films showed improved activity on a per cobalt basis the material had poor interactions with the substrate, resulting in detachment of the COF films over time. We reasoned that this challenge could be overcome by growing oriented thin films of COFs on a more ordered surface. In addition to an improved interaction with the electrode surface, oriented thin films have also been shown to facilitate redox processes in COF materials.[44] Accordingly, we chose highly ordered pyrolytic graphite (HOPG) as our electrode material. Oriented thin films were grown by adding the substrate to the reaction mixture containing [5,10,15,20-tetrakis(4-aminophenyl)porphinato]-cobalt, Co(TAP), and 1,4-benzenedicarboxaldehyde (BDA) (Figure 2). The crystallinity and preferred orientation of the films in respect to the substrate were confirmed by grazing incidence wide-angle X-ray scattering (GIWAXS) (Figure 2a). The diffraction pattern of the oriented thin films of COF-366-Co confirmed the formation of the expected structure (Figure 2d). Contrary to our expectations, the COF layers did not grow coplanar to the electrode surface but orient perpendicular to the graphite layers (Figure 2c). Scanning electron microscopy showed films of uniform thickness of ~250 nm (Figure 2b).

Electrochemical experiments were carried out in 0.5 M potassium bicarbonate aqueous buffer at pH 7.2 and controlled potential electrolysis was performed under an applied potential of −0.67 (vs. RHE). The oriented thin films of COF-366-Co exhibited significantly improved catalytic performance on a per cobalt basis with current densities for the formation of CO of 45 mA/mg cobalt and a faradaic efficiency of 87% which constitutes a 9-fold improvement over the microcrystalline COF powders. While the reactivity of the films grown on glassy carbon initially showed a similar performance, the oriented films show a significantly improved long-term stability for more than 12 h (Figure 2e). With the optimized morphology at hand, we chose to advance a step further and utilize the unique features of our catalyst system: (i) the high degree of electronic communication throughout the whole framework[48] and (ii) the organic backbone of the structure which allows for covalent modification.[9,49,50] The proposed mechanism for CO_2 reduction with cobalt porphyrin suggests that in a first step cobalt(II) gets reduced to cobalt(I) (Section S2).[43] To facilitate this step, we decided to introduce electron-withdrawing functional groups onto the linker of the COF to take away electron density from the cobalt center and make it more prone to reduction.[51]

Covalent Functionalization of COF-366-Co. We thus set out to make a series of COFs with systematically incorporated functionality, namely COF-366-Co, COF-366$(OMe)_2$-Co, COF-366-F-Co and COF-366-$(F)_4$-Co (Figure 1), to determine the COF with the optimal amount of electron withdrawing groups and maximize the reactivity at a given overpotential. The synthesis of these frameworks was carried out analogous to the synthesis of the parent framework COF-366-Co. Powder X-ray diffraction confirmed that the space group and the metrics of the structures remained essentially unaltered (Sections S3 and S4). The films of all COFs were crystalline and the grazing incidence wide-angle X-ray scattering of all structures confirmed the same orientation with respect to the substrate as described above for COF-366-Co (Sections S3 and S4). To confirm that the effects that we measure in the COFs are due to differences in the electronic nature and not a result of different affinities of the framework itself for CO_2, we carried out CO_2 sorption on all of the studied materials. The materials all displayed a comparable uptake of CO_2 at 295 K (23.5−27.4 $cm^3\ cm^{-1}$). To confirm that the affinity for CO_2 of the different frameworks is also similar we measured CO_2 sorption at different temperatures to derive isosteric heat of adsorption (Q_{st}) values which turned out to be the same for all measured materials (24.6−24.1 kJ mol^{-1}) (Table 1; Section S5 and S8).

Table 1. Pore Size Distribution (PSD), BET Surface Area (A_{BET}), CO_2 Uptake, and Isosteric Heat of Adsorption (Q_{st}) Values for the Binding of CO_2 for the COF Catalysts

material	PSD (Å)[a]	A_{BET} ($m^2\ g^{-1}$)[b]	CO_2 uptake ($cm^3\ g^{-1}$)[c]	Q_{st} (kJ mol^{-1})[d]
COF-366-Co	10−18	1700	23.4	24.6
COF-366-$(OMe)_2$-Co	8−18	867	24.2	24.4
COF-366−F-Co	10−18	1901	27.0	24.2
COF-366-$(F)_4$-Co	8−16	832	27.4	24.1

[a]Determined by fitting of the adsorption branch using quenched solid state density functional theory (QSDFT) cylindrical/slit pore model on the absorption branch of the isotherm. [b]Calculated using the BET method from the nitrogen sorption data of the activated samples at 77 K. [c]Uptake at 800 Torr and 298 K, the conditions under which we carry out the catalysis. [d]Calculated from pure component isotherms using Henry's law.

X-ray Absorption Spectroscopy. To further probe the effect of the introduced groups on the catalytically active cobalt site we turned to X-ray absorption spectroscopy (XAS) on the cobalt L-edge. Such a measurement would directly determine whether or not modification does indeed cause a change in the electronic structure of the metal center. The metal L-edge spectra feature transitions from 2p core electrons into unoccupied 3d states.[52−54] The resulting spectrum imparts information regarding the formal oxidation state, symmetry, and extent of electronic delocalization of the probed element.[55−57] Considering the fact that the d-orbitals are the orbitals that are principally relevant to the catalytic activity of the porphyrin metal center, L-edge absorption measurements yield direct information on the effect of the substituents on the electronic structure of the catalyst. The L3-edge spectra of the different COFs and a series of molecular porphyrin model systems {Co(TIP) = [5,10,15,20-tetrakis(1-*N*-benzylideneaniline)porphinato]cobalt, Co(THP) = [5,10,15,20-tetrakis(4-hydroxyphenyl)porphinato]cobalt, Co-(TCPP) = [5,10,15,20-tetrakis(4-carboxyphenyl)porphinato]-cobalt, Co(TAP)} are illustrated in Figure 3a, b, respectively. Immediately noticeable is the increasing intensity of peaks at 777 and 779 eV for the porphyrin model with increasing electron withdrawing character of the functional groups. The XAS spectra of the COFs also change depending on the functional group that is present on the linker. Comparison of the data to theoretically modeled spectra by introducing inductive effects from a hypothetical square planar ligand field confirmed an increasing electron withdrawing effect of the linker on the cobalt site in the order: COF-366-Co, COF-366-$(OMe)_2$-Co, COF-366-$(F)_4$-Co, and COF-366-F-Co (Figure 3c−g; Section S6). The fact that the differences in electron withdrawing character on the cobalt center do not follow the expected trend according to basic inductive effect considerations is giving credence to the importance of this study for

DOI: 10.1021/jacs.7b11940
J. Am. Chem. Soc. 2018, 140, 1116−1122

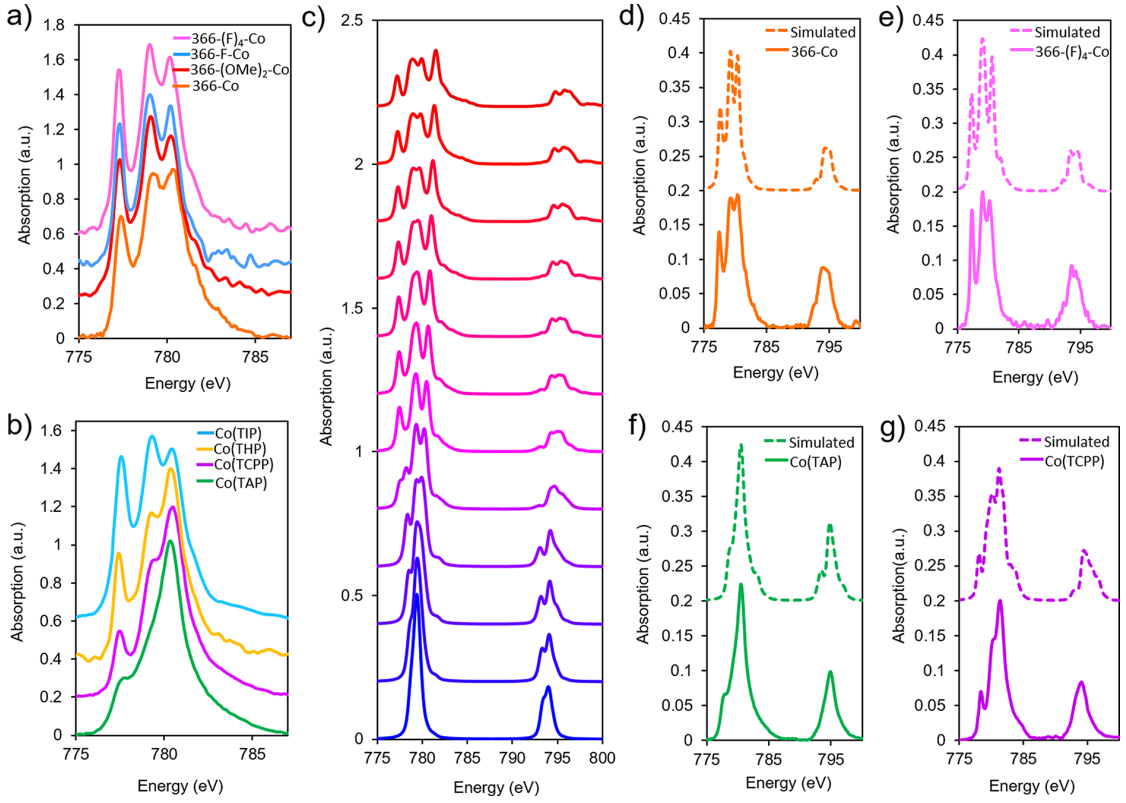

Figure 3. XAS Co L-edge spectroscopy. (a) Spectra of COF-366-Co and derivatives and (b) various molecular cobalt porphyrin complexes. In both cases, the spectra are stacked in order of increasing negative inductive effect. (c) Changes in the theoretical spectrum of a cobalt(II) ion are shown for a hypothetical increasing electron-withdrawing ligand field where the negative inductive effect of the ligand field increases from bottom (blue) to top (red). Obtained XAS cobalt L-edge spectra for (d) COF-366-Co, (e) COF-366-$(F)_4$-Co, (f) Co(TAP), and (g) Co(TCPP) are in good agreement with their respective simulated patterns.

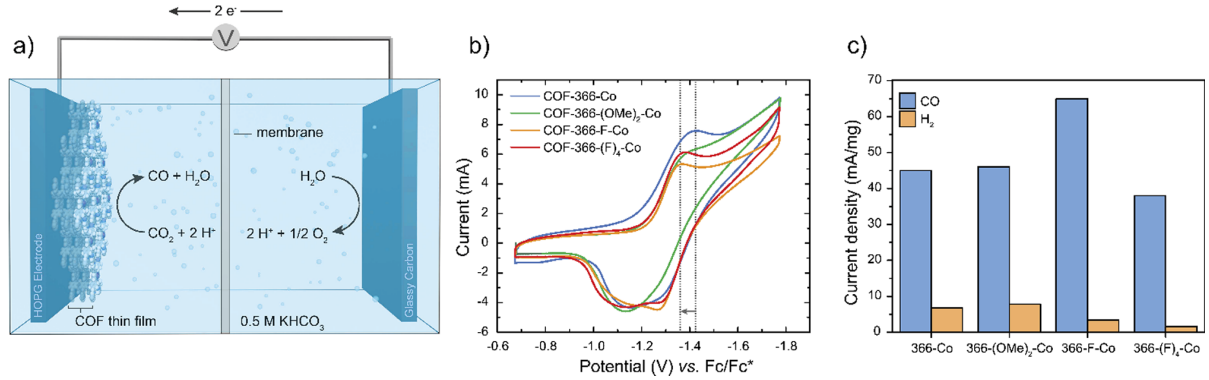

Figure 4. Electrochemical characterization of the COFs. (a) Illustration of the electrolysis cell and the two respective half reactions. (b) Cyclic voltammogramms of COF-366-Co, COF-366-$(OMe)_2$-Co, COF-366-F-Co, and COF-366-$(F)_4$-Co in *N*,*N*-dimethylformamide with tetrabutylammonium hexafluorophosphate as the electrolyte. (c) Current densities per milligram of cobalt in the different COF catalysts under an applied potential of −0.67 V vs. RHE in 0.5 M aqueous potassium bicarbonate buffer.

accurate structure−property relationships of the catalysts. Furthermore, it is noteworthy that COF-366-Co itself when compared to the starting material Co(TAP) does in fact display a stronger electron withdrawing effect on the cobalt center which might be a possible explanation for the significantly lower reactivity of the molecular catalyst in comparison to the COF (Figure 3d, f; Section S6).

Electrochemical Characterization. To verify that the differences in electronic structure translate into modified electrochemical properties, we measured cyclic voltammograms of the different compounds in *N*,*N*-dimethylformamide with tetrabutylammonium hexafluorophosphate as the electrolyte, which show that the potential of the cathodic wave does indeed shift from −1.425 V vs. ferrocene/ferrocenium (Fc/Fc^+) for COF-366-Co up to −1.380 V vs. Fc/Fc^+ for COF-366-F-Co

DOI: 10.1021/jacs.7b11940
J. Am. Chem. Soc. 2018, 140, 1116−1122

(Figure 4b). The trend here tracks to what is observed in the XAS spectra, which confirms the unexpected order of electron withdrawing effects in the different COF materials. It should be noted that the CVs were obtained from powder samples deposited on a porous carbon cloth as opposed to COF thin films and that the resulting current was not normalized by the weight of the material (Figure 4b). Consequently, we further tested the reactivity of the different COF catalysts to evaluate differences in current at a given potential. Controlled potential electrolyses were carried out in aqueous solution at −0.67 V vs reversible hydrogen electrode (RHE) and the different catalysts show significant differences in reactivity. As expected, the electron withdrawing character observed by XAS and cyclic voltammetry improves the catalytic behavior of the framework and the current density for CO formation increases from 45 mA mg^{-1} for COF-366-Co to 46 mA mg^{-1} COF-366-$(OMe)_2$-Co up to 65 mA mg^{-1} for COF-366−F-Co. COF-366-$(F)_4$-Co does not perfectly represent the trend as it is the second most electron-withdrawing material but displays the lowest reactivity. We attribute this observation to the higher hydrophobicity of the framework and resulting decreased access of electrolyte to the active sites (Figure 4c).[58−60]

CONCLUSION

The findings of this study illustrate the promise of covalent organic frameworks as an emerging class of materials for supporting catalysis with molecular-level control of both physical and electronic structure. We demonstrated that optimizing the morphology of COFs and growing them as oriented thin films significantly improves the catalytic activity of the material compared to bulk samples. More importantly, reticular electronic tuning of the catalytically active cobalt sites was used to optimize the material for high activity and selectivity by facile functionalization of the reticular parent structure with electron-withdrawing groups. In this regard, X-ray absorption spectroscopy on the metal L-edge has proved a useful tool for the direct observation of the effect of framework functionalization on the metal center. The importance of the spectroscopic evidence is highlighted by the fact that the differences in the electronic character of the active sites do not follow the expected trend according to basic inductive effect considerations. We anticipate the modularity of COF systems through reticular synthesis, combined with the ability to engender electronic communication between reticulated active sites and the surrounding framework, will promote further opportunities for a broad array of catalytic transformations and related applications.

ASSOCIATED CONTENT

Supporting Information

The Supporting Information is available free of charge on the ACS Publications website at DOI: 10.1021/jacs.7b11940.

Synthetic protocols, powder X-ray diffraction analysis, structural modeling, and porosity evaluation of the different COFs, as well as details concerning the X-ray absorption spectroscopy and CO_2 sorption (PDF)

AUTHOR INFORMATION

Corresponding Authors

*E-mail: yaghi@berkeley.edu
*E-mail: chrischang@berkeley.edu

ORCID

Christian S. Diercks: 0000-0002-7813-0302
Song Lin: 0000-0002-8880-6476
Eugene A. Kapustin: 0000-0003-4095-9729
Yingbo Zhao: 0000-0002-6289-7015
Christopher J. Chang: 0000-0001-5732-9497
Omar M. Yaghi: 0000-0002-5611-3325

Author Contributions

†C.S.D. and S.L. contributed equally.

Notes

The authors declare no competing financial interest.

ACKNOWLEDGMENTS

Financial support for COF research in the O.M.Y. laboratory was provided by the Army Research Office for the Multi-disciplinary University Research Initiatives award WG11NF-15-1-0047 for the synthesis and characterization of 2D-COFs and the Center for Gas Separations Relevant to Clean Energy Technologies, an Energy Frontier Research Center funded by the U.S. Department of Energy, Office of Science, Basic Energy Sciences (DESC0001015), for gas adsorption studies. C.S.D. acknowledges the KAVLI foundation for a KAVLI ENSI graduate student fellowship and Ms. Y. Liu and Dr. M.J. Kalmutzki for helpful discussions. Financial support for energy catalysis in the C.J.C. laboratory, particularly molecular and electrochemical studies, is provided by the U.S. Department of Energy/Lawrence Berkeley National Laboratory (LBNL) Grant 101528-002. C.J.C. is an Investigator with the Howard Hughes Medical Institute and a CIFAR Senior Fellow. E.M.N. thanks the NSF for a graduate fellowship. N.K. gratefully acknowledges the Royal Society Newton International Fellowship. Work at the Molecular Foundry was supported by the Office of Science, Office of Basic Energy Sciences, of the U.S. Department of Energy under Contract DE-AC02-05CH11231. The Advanced Light Source is supported by the Director, Office of Science, Office of Basic Energy Sciences, of the U.S. Department of Energy under Contract DE-AC02-05CH11231. We acknowledge Prof. Peidong Yang for helpful input into this project.

REFERENCES

(1) Diercks, C. S.; Yaghi, O. M. *Science* **2017**, *355*, 923.
(2) Huang, N.; Wang, P.; Jiang, D. *Nat. Rev. Mater.* **2016**, *1*, 16068.
(3) Cote, A. P.; Benin, A. I.; Ockwig, N. W.; O'Keeffe, M.; Matzger, A. J.; Yaghi, O. M. *Science* **2005**, *310*, 1166.
(4) Bisbey, R. P.; Dichtel, W. R. *ACS Cent. Sci.* **2017**, *3*, 533.
(5) Segura, J. L.; Mancheño, M. J.; Zamora, F. *Chem. Soc. Rev.* **2016**, *45*, 5635.
(6) Baldwin, L. A.; Crowe, J. W.; Pyles, D. A.; McGrier, P. L. *J. Am. Chem. Soc.* **2016**, *138*, 15134.
(7) Ascherl, L.; Sick, T.; Margraf, J. T.; Lapidus, S. H.; Calik, M.; Hettstedt, C.; Karaghiosoff, K.; Döblinger, M.; Clark, T.; Chapman, K. W.; et al. *Nat. Chem.* **2016**, *8*, 310.
(8) El-Kaderi, H. M.; Hunt, J. R.; Mendoza-Cortés, J. L.; Côté, A. P.; Taylor, R. E.; O'Keeffe, M.; Yaghi, O. M. *Science* **2007**, *316*, 268.
(9) Ding, S.-Y.; Gao, J.; Wang, Q.; Zhang, Y.; Song, W.-G.; Su, C.-Y.; Wang, W. *J. Am. Chem. Soc.* **2011**, *133*, 19816.
(10) Doonan, C. J.; Tranchemontagne, D. J.; Glover, T. G.; Hunt, J. R.; Yaghi, O. M. *Nat. Chem.* **2010**, *2*, 235.
(11) Xu, H.; Tao, S.; Jiang, D. *Nat. Mater.* **2016**, *15*, 722.
(12) Xu, H.; Gao, J.; Jiang, D. *Nat. Chem.* **2015**, *7*, 905.
(13) Lohse, M. S.; Stassin, T.; Naudin, G.; Wuttke, S.; Ameloot, R.; De Vos, D.; Medina, D. D.; Bein, T. *Chem. Mater.* **2016**, *28*, 626.
(14) Fang, Q.; Wang, J.; Gu, S.; Kaspar, R. B.; Zhuang, Z.; Zheng, J.; Guo, H.; Qiu, S.; Yan, Y. *J. Am. Chem. Soc.* **2015**, *137*, 8352.

DOI: 10.1021/jacs.7b11940
J. Am. Chem. Soc. 2018, 140, 1116−1122

(15) Sun, Q.; Aguila, B.; Perman, J.; Earl, L. D.; Abney, C. W.; Cheng, Y.; Wei, H.; Nguyen, N.; Wojtas, L.; Ma, S. *J. Am. Chem. Soc.* **2017**, *139*, 2786.
(16) Lin, S.; Diercks, C. S.; Zhang, Y.-B.; Kornienko, N.; Nichols, E. M.; Zhao, Y.; Paris, A. R.; Kim, D.; Yang, P.; Yaghi, O. M.; Chang, C. J. *Science* **2015**, *349*, 1208.
(17) Kornienko, N.; Zhao, Y.; Kley, C. S.; Zhu, C.; Kim, D.; Lin, S.; Chang, C. J.; Yaghi, O. M.; Yang, P. *J. Am. Chem. Soc.* **2015**, *137*, 14129.
(18) Hod, I.; Sampson, M. D.; Deria, P.; Kubiak, C. P.; Farha, O. K.; Hupp, J. T. *ACS Catal.* **2015**, *5*, 6302.
(19) Costentin, C.; Robert, M.; Savéant, J.-M. *Chem. Soc. Rev.* **2013**, *42*, 2423.
(20) Kumar, B.; Llorente, M.; Froehlich, J.; Dang, T.; Sathrum, A.; Kubiak, C. P. *Annu. Rev. Phys. Chem.* **2012**, *63*, 541.
(21) Keith, J. A.; Grice, K. A.; Kubiak, C. P.; Carter, E. A. *J. Am. Chem. Soc.* **2013**, *135*, 15823.
(22) Sampson, M. D.; Nguyen, A. D.; Grice, K. A.; Moore, C. E.; Rheingold, A. L.; Kubiak, C. P. *J. Am. Chem. Soc.* **2014**, *136*, 5460.
(23) Beley, M.; Collin, J.-P.; Ruppert, R.; Sauvage, J.-P. *J. Chem. Soc., Chem. Commun.* **1984**, 1315.
(24) Hawecker, J.; Lehn, J.-M.; Ziessel, R. *J. Chem. Soc., Chem. Commun.* **1984**, 328.
(25) Froehlich, J. D.; Kubiak, C. P. *Inorg. Chem.* **2012**, *51*, 3932.
(26) Behar, D.; Dhanasekaran, T.; Neta, P.; Hosten, C.; Ejeh, D.; Hambright, P.; Fujita, E. *J. Phys. Chem. A* **1998**, *102*, 2870.
(27) Collin, J. P.; Jouaiti, A.; Sauvage, J. P. *Inorg. Chem.* **1988**, *27*, 1986.
(28) Thoi, V. S.; Kornienko, N.; Margarit, C. G.; Yang, P.; Chang, C. J. *J. Am. Chem. Soc.* **2013**, *135*, 14413.
(29) Thoi, V. S.; Chang, C. J. *Chem. Commun.* **2011**, *47*, 6578.
(30) Appel, A. M.; Bercaw, J. E.; Bocarsly, A. B.; Dobbek, H.; DuBois, D. L.; Dupuis, M.; Ferry, J. G.; Fujita, E.; Hille, R.; Kenis, P. J.; et al. *Chem. Rev.* **2013**, *113*, 6621.
(31) Fisher, B. J.; Eisenberg, R. *J. Am. Chem. Soc.* **1980**, *102*, 7361.
(32) Beley, M.; Collin, J. P.; Ruppert, R.; Sauvage, J. P. *J. Am. Chem. Soc.* **1986**, *108*, 7461.
(33) Rosen, B. A.; Salehi-Khojin, A.; Thorson, M. R.; Zhu, W.; Whipple, D. T.; Kenis, P. J.; Masel, R. I. *Science* **2011**, *334*, 643.
(34) Kuhl, K. P.; Cave, E. R.; Abram, D. N.; Jaramillo, T. F. *Energy Environ. Sci.* **2012**, *5*, 7050.
(35) Li, C. W.; Kanan, M. W. *J. Am. Chem. Soc.* **2012**, *134*, 7231.
(36) Kim, D.; Resasco, J.; Yu, Y.; Asiri, A. M.; Yang, P. *Nat. Commun.* **2014**, *5*, 4948.
(37) Costentin, C.; Passard, G.; Robert, M.; Savéant, J.-M. *Proc. Natl. Acad. Sci. U. S. A.* **2014**, *111*, 14990.
(38) Costentin, C.; Drouet, S.; Robert, M.; Savéant, J.-M. *Science* **2012**, *338*, 90.
(39) Rao, H.; Schmidt, L. C.; Bonin, J.; Robert, M. *Nature* **2017**, *548*, 74.
(40) Azcarate, I.; Costentin, C.; Robert, M.; Savéant, J.-M. *J. Am. Chem. Soc.* **2016**, *138*, 16639.
(41) Bhugun, I.; Lexa, D.; Savéant, J.-M. *J. Am. Chem. Soc.* **1996**, *118*, 1769.
(42) Collin, J.; Sauvage, J. P. *Coord. Chem. Rev.* **1989**, *93*, 245.
(43) Leung, K.; Nielsen, I. M.; Sai, N.; Medforth, C.; Shelnutt, J. A. *J. Phys. Chem. A* **2010**, *114*, 10174.
(44) DeBlase, C. R.; Silberstein, K. E.; Truong, T.-T.; Abruña, H. D.; Dichtel, W. R. *J. Am. Chem. Soc.* **2013**, *135*, 16821.
(45) Rogge, S. M.; Bavykina, A.; Hajek, J.; Garcia, H.; Olivos-Suarez, A. I.; Sepúlveda-Escribano, A.; Vimont, A.; Clet, G.; Bazin, P.; Kapteijn, F.; et al. *Chem. Soc. Rev.* **2017**, *46*, 3134.
(46) Stavitski, E.; De Groot, F. M. *Micron* **2010**, *41*, 687.
(47) Ilavsky, J. *J. Appl. Crystallogr.* **2012**, *45*, 324.
(48) Wan, S.; Gándara, F.; Asano, A.; Furukawa, H.; Saeki, A.; Dey, S. K.; Liao, L.; Ambrogio, M. W.; Botros, Y. Y.; Duan, X.; et al. *Chem. Mater.* **2011**, *23*, 4094.
(49) Huang, N.; Krishna, R.; Jiang, D. *J. Am. Chem. Soc.* **2015**, *137*, 7079.
(50) Waller, P. J.; Lyle, S. J.; Osborn Popp, T. M.; Diercks, C. S.; Reimer, J. A.; Yaghi, O. M. *J. Am. Chem. Soc.* **2016**, *138*, 15519.
(51) Zhang, X.; Wu, Z.; Zhang, X.; Li, L.; Li, Y.; Xu, H.; Li, X.; Yu, X.; Zhang, Z.; Liang, Y.; Wang, H. *Nat. Commun.* **2017**, *8*, 14675.
(52) Leapman, R.; Grunes, L.; Fejes, P. *Phys. Rev. B: Condens. Matter Mater. Phys.* **1982**, *26*, 614.
(53) Cressey, G.; Henderson, C.; Van der Laan, G. *Phys. Chem. Miner.* **1993**, *20*, 111.
(54) De Groot, F.; Hu, Z.; Lopez, M.; Kaindl, G.; Guillot, F.; Tronc, M. *J. Chem. Phys.* **1994**, *101*, 6570.
(55) Fanetti, M.; Calzolari, A.; Vilmercati, P.; Castellarin-Cudia, C.; Borghetti, P.; Di Santo, G.; Floreano, L.; Verdini, A.; Cossaro, A.; Vobornik, I.; et al. *J. Phys. Chem. C* **2011**, *115*, 11560.
(56) Hibberd, A. M.; Doan, H. Q.; Glass, E. N.; De Groot, F. M.; Hill, C. L.; Cuk, T. *J. Phys. Chem. C* **2015**, *119*, 4173.
(57) Kroll, T.; Aristov, V. Y.; Molodtsova, O.; Ossipyan, Y. A.; Vyalikh, D.; Buchner, B.; Knupfer, M. *J. Phys. Chem. A* **2009**, *113*, 8917.
(58) Chen, T.-H.; Popov, I.; Zenasni, O.; Daugulis, O.; Miljanić, O. Š. *Chem. Commun.* **2013**, *49*, 6846.
(59) Deria, P.; Mondloch, J. E.; Tylianakis, E.; Ghosh, P.; Bury, W.; Snurr, R. Q.; Hupp, J. T.; Farha, O. K. *J. Am. Chem. Soc.* **2013**, *135*, 16801.
(60) Chui, S. S.-Y.; Lo, S. M.-F.; Charmant, J. P. H.; Orpen, A. G.; Williams, I. D. *Science* **1999**, *283*, 1148.

DOI: 10.1021/jacs.7b11940
J. Am. Chem. Soc. 2018, 140, 1116−1122